EFFECTS OF THERMAL DIFFUSION AND DIFFUSION THERMO ON MHD COMBINED CONVECTION AND MASS TRANSFER PAST A VERTICAL POROUS PLATE EMBEDDED IN A POROUS MEDIUM WITH HEAT GENERATION, THERMAL RADIATION, nth ORDER CHEMICAL REACTION AND VISCOUS DISSIPATION

A.W. Ogunsola[1] · P.O. Olanrewaju[2] · F.I. Alao[3] · R. Osinowo[2] · O. J. Fenuga[4]

[1]Department of Pure and Applied Mathematics, Ladoke Akintola University of Technology, Ogbomoso, Nigeria

[2]Department of Mathematical Sciences, Oduduwa University, Ipetumodu, Ile-Ife, Nigeria

[3]Department of Mathematical Sciences, Federal University of Technology, Akure, Nigeria

[4]Department of Mathematics, University of Lagos, Lagos, Nigeria

Abstract This paper focuses on the effects of Soret, Dufour, heat generation, radiation, order of chemical reaction and viscous dissipation on a steady combined free-force convective and mass transfer flow of a viscous incompressible electrically conducting and radiating fluid over an isothermal semi-infinite vertical porous flat plate embedded in a porous medium. The partial differential equations governing the problem have been transformed by a similarity transformation into a system of ordinary differential equations which are solved numerically by using the sixth-order of Runge-Kutta technique alongside with shooting method. The behavior of the velocity, temperature, concentration, skin-friction coefficient, Nusselt number and Sherwood number for variations in the governing thermo physical embedded parameters are computed, analyzed and discussed.

Keywords Soret and Dufour, Thermal radiation, nth order chemical reaction, Heat generation, Heat and mass transfer, Viscous dissipation.

Introduction

If the gradients of two stratifying agencies, such as heat and salt, having different diffusivities are simultaneously present in a fluid layer, a variety of interesting convective phenomena can occur which are not possible in a single component fluid. Convection in a fluid layer with two or more stratifying agencies has been the subject of extensive theoretical and experimental investigations in the last few decades. Excellent reviews of these studies have been reported by Turner [1–3], Huppert and Turner [4] and Platten and Legros [5]. The interest in the study of two or multi-component convection has developed as a result of the marked difference between single component and multicomponent systems. In contrast to single component system, convection sets is even when density decreases with height, that is, when the basic state is hydrostatically stable. The double diffusive convection is of importance in various fields such as high quality crystal production, liquid gas storage, oceanography, and production of pure medication, solidification of molten alloys, and exothermally heated lakes and magmas. Convection in a two-component fluid is characterized by well-mixed convecting layers, which are separated by relatively sharp density steps. These steps may be of the 'finger' or 'diffusive' kind and both types of interface must enable a net release of potential energy preferentially transporting the destabilizing property. Salt fingers will occur when warm salty fluid overlies cooler fresher fluid and diffusive instability will occur when warm salty fluid underlies the fresh cooler

fluid. In two component system, in the absence of cross-diffusion, instability can occur only if, at least one of the components is destabilizing. However, in the presence of cross-diffusions produced by the simultaneous interference of two transport properties e.g., Soret and Dufour effects the situations may be quite different [6–8]. Typically, the energy transport is described adequately by Fourier diffusion and the mass transport by Fickian diffusion alone. Otherwise, several investigators [9–12] have shown both analytically and experimentally that both Soret and Dufour effects can be important contributions to the total mass and energy transfer, respectively. The thermal-diffusion (Soret) effect, for instance, has been utilized for isotope separation, and in mixture between gases with very light molecular weight (H_2, He) and of medium molecular weight (N_2, air) the diffusion thermo (Dufour) effects was found to be of order of considerable magnitude such that it cannot be ignored [13]. In view of the importance of above-mentioned effects Atimtay and Gill [14] have shown that Soret and Dufour diffusion to be appreciable for convection on a rotating disc. Weaver and Viskanta [15] studied the influence of species interdiffusion, Soret and Dufour effects on the natural convection heat and mass transfer in a cavity due to combined temperature and concentration gradients. They have shown that contributions to the total mass flux through the cavity due to Soret diffusion can be as much as 10–15% and energy transfer due to Dufour effects can be appreciable compared to heat conduction. Kafoussias and Williams [16] studied thermal-diffusion and diffusion-thermo effects on mixed free-forced convective and mass transfer boundary layer flow with temperature-dependent viscosity. Thermal convection in a binary fluid driven by the Soret and Dufour effects has been investigated by Knobloch [17]. He has shown that equations are identical to the thermosolutal problem except for a relation between the thermal and solute Rayleigh numbers. Osalusi et al. [18] studied the thermal-diffusion and diffusion-thermo effects on combined heat and mass transfer of a steady MHD convective and slip flow due to a rotating disk with viscous dissipation and Ohmic heating. Beg et al. [19] examined the numerical study of free convection magnetohydrodynamic heat and mass transfer from a stretching surface to a saturated porous medium with Soret and Dufour effects. Similarly, similarity solution in MHD: effects of thermal diffusion and diffusion thermo on free convective heat and mass transfer over a stretching surface considering suction or injection was studied by Afify [20]. Recently, Hayat et al. [21] examined heat and mass transfer for Soret and Dufour's effect on mixed convection boundary layer flow over a stretching vertical surface in a porous medium filled with a viscoelastic fluid.

However, the interaction of radiation with mass transfer in an combined convection flow in the presence of Soret and Dufour's effect has received little attention. Hence, an attempt is made to analyze the effects of thermal diffusion and diffusion thermo on MHD combined convection and mass transfer past a vertical porous plate embedded in a porous medium with heat generation, thermal radiation, nth order chemical reaction and viscous dissipation by extending Reddy and Reddy [22] to include Dufour, Soret, viscous dissipation and nth order chemical reaction. The equations of continuity, linear momentum, energy and diffusion, which govern the flow field, are solved by Runge-Kutta sixth order method along with shooting technique. The behavior of the velocity, temperature, concentration, skin-friction, Nusselt number and Sherwood number have been discussed for variations in the embedded flow parameters that governs the flow field.

Problem statement

A two dimensional steady combined free-forced convective and mass transfer flow of a viscous incompressible electrically conducting and radiating fluid over an isothermal semi-infinite vertical porous flat plate embedded in a porous medium in the presence of thermal radiation, nth order chemical reaction with Dufour and Soret effects is considered. The flow is assumed to be in the *x*-direction, which is taken along the vertical plate in the upward direction and *y*-axis is taken to be normal to the plate. A temperature dependent heat source is assumed to be present in the flow. The fluid is assumed to be gray, emitting and absorbing radiation but non-scattering. The transverse applied magnetic field and magnetic Reynolds number are assumed to be very small, so that the induced magnetic field is negligible. The surface of the plate is maintained at a uniform constant temperature T_w and a uniform constant concentration C_w of a foreign fluid, which are higher than the corresponding value T_∞ and C_∞ respectively, sufficiently far away from the flat surface. It is also assumed that the free stream velocity U_∞, parallel to the vertical plate, is constant. Then, under the usual Boussinesq's approximation, in the absence of an input electric field, the governing boundary layer equations are

$$\frac{\partial u}{\partial x} + \frac{\partial v}{\partial y} = 0$$

(1)

$$u\frac{\partial u}{\partial x} + v\frac{\partial u}{\partial y} = v\frac{\partial^2 u}{\partial y^2} + g\beta_T(T - T_\infty) + g\beta_C(C - C_\infty) - \frac{\sigma B_o^2}{\rho}u - \frac{\upsilon}{K}u,$$

(2)

$$u\frac{\partial T}{\partial x} + v\frac{\partial T}{\partial y} = \frac{k}{\rho c_p}\frac{\partial^2 T}{\partial y^2} - \frac{1}{\rho c_p}\frac{\partial q_r}{\partial y} + \frac{Q_0}{\rho c_p}(T - T_\infty) + \frac{\mu}{\rho c_p}\left(\frac{\partial u}{\partial y}\right)^2 + \frac{D_m k_T}{c_s c_p}\frac{\partial^2 C}{\partial y^2}$$

(3)

$$u\frac{\partial C}{\partial x} + v\frac{\partial C}{\partial y} = D_m\frac{\partial^2 C}{\partial y^2} - R(C - C_\infty)^n + \frac{D_m k_T}{T_m}\frac{\partial^2 T}{\partial y^2}$$

(4)

Where u, v are the velocity components in x- and y- directions respectively, ν- the kinematic viscosity, g- the acceleration due to gravity, β_T – the coefficient of volume expansion, β_C – the volumentric coefficient of expansion with concentration, T – the temperature of the fluid in the boundary layer, T_∞ – the temperature of the fluid far away from the plate, C – the species concentration in the boundary layer, C_∞ – the species concentration in the fluid far away from the plate, R – the chemical reaction coefficient, μ – the dynamic viscosity of the fluid, σ – the electrical conductivity of the fluid, B_0 – the magnetic induction, ρ – the density of the fluid, K – the permeability of the porous medium, k – the thermal conductivity, c_p – the specific heat at constant pressure, q_r – the radiation heat flux, Q_0 – the heat generation constant, D_m – the coefficient of mass diffusivity, c_s – the concentration susceptibility, T_m – the mean fluid temperature and k_T - the thermal-diffusion ratio.

The boundary conditions for the velocity, temperature and concentration fields are

$$u=0, \quad v=v_w(x), \quad T=T_w, \quad C=C_w \quad at \quad y=0$$
$$u=U_\infty, \quad T=T_\infty, \quad C=C_\infty \quad as \quad y\to\infty.$$

(5)

By using the Rosseland approximation (see Brewster [23]), the radiative heat flux is given by

$$q_r = -\frac{4\sigma^*}{3k^*}\frac{\partial T^4}{\partial y},$$

(6)

where σ^* is the Stefan-Boltzmann constant and k^* - the mean absorption coefficient. It should be noted that by using the Rosseland approximation, the present analysis is limited to optically thick fluids. If temperature differences within the flow are sufficiently small, then equation (6) can be linearized by expanding T^4 into the Taylor series about T_∞, which after neglecting higher order terms takes the form

$$T^4 \cong 4T_\infty^3 T - 3T_\infty^4.$$

(7)

In order to obtain the similarity solution of the problem, the following non-dimensional variables are introduced.

$$\eta = y\sqrt{\frac{U_\infty}{\upsilon x}}, \ \psi = \sqrt{\upsilon x U_\infty}\, f(\eta), \ \ \theta(\eta) = \frac{T - T_\infty}{T_w - T_\infty}, \ \phi(\eta) = \frac{C - C_\infty}{C_w - C_\infty}, \ u = \frac{\partial \psi}{\partial y},$$

$$v = -\frac{\partial \psi}{\partial x}, \ Gt = \frac{g\beta(T_w - T_\infty)x^3}{\upsilon^2}, G_C = \frac{g\beta^*(C_w - C_\infty)x^3}{\upsilon^2}, M = \frac{\sigma B_0^2 x}{\rho U_\infty}, \text{Re} = \frac{U_\infty x}{\upsilon},$$

$$g_s = \frac{Gt}{\text{Re}^2}, \ g_c = \frac{G_C}{\text{Re}^2}, \Pr = \frac{\upsilon c_p}{k}, Q = \frac{Q_0 x}{\rho c_p U_\infty}, \ Sc = \frac{\upsilon}{D_m}, K = \frac{\upsilon x}{K' U_\infty}, Ra = \frac{4\sigma^* T_\infty^3}{k^* k}, \quad (8)$$

$$Ec = \frac{\mu U_\infty^2}{\rho c_p \sqrt{\upsilon x}}, \ Df = \frac{D_m k_T}{c_s c_p}\frac{(C_w - C_\infty)}{(T_w - T_\infty)}, Sr = \frac{D_m k_T \rho c_p}{T_m k}\frac{(T_w - T_\infty)}{(C_w - C_\infty)}, \lambda = \frac{R(C_w - C_\infty)^{n-1}}{v_w(x)}$$

Where ψ is the stream function, θ- the non-dimensional temperature function, φ- the non-dimensional concentration, Gt- the thermal Grashof number, G_C – the mass Grashof number, M – the magnetic field parameter, Re – the Reynolds number, g_s – the temperature buoyancy parameter, g_c – the mass buoyancy parameter, Pr – the Prandtl number, Q – the heat generation parameter, Sc – the Schmidt number, K – the permeability parameter, Ra – the radiation parameter, Ec – the Eckert number, Df – the Dufour number, Sr – the Soret number, and λ – the chemical reaction parameter.

In view of equations (7) and (8), the equations (2)-(4) reduces to

$$f''' + \frac{1}{2}ff'' + g_s\theta + g_c\phi - (M + K)f' = 0, \tag{9}$$

$$\left(1 + \frac{4}{3}Ra\right)\theta'' + \frac{1}{2}\Pr f\theta' + \Pr Q\theta + \Pr Ec(f'')^2 + Df\Pr\phi'' = 0, \tag{10}$$

$$\phi'' + \frac{1}{2}Scf\phi' - Sc\lambda\phi^n + ScSr\theta'' = 0, \tag{11}$$

$$f(0) = fw, \ \ f'(0) = 0, \ \ \theta(0) = 1, \ \ \phi(0) = 1, \tag{12}$$

$$f'(\infty) = 1, \ \ \ \theta(\infty) = 0, \ \ \phi(\infty) = 0. \tag{13}$$

Where $fw = -2v_w(x)\sqrt{\dfrac{x}{\upsilon U_\infty}}$ is the suction parameter.

The physical quantities, known as the skin-friction, the Nusselt number and the Sherwood number can be written as

$$c_f = 2(\text{Re})^{-\frac{1}{2}} f''(0), \tag{14}$$

$$Nu = -(\text{Re})^{\frac{1}{2}} \theta'(0), \tag{15}$$

$$Sh = -(\text{Re})^{\frac{1}{2}} \phi'(0), \tag{16}$$

where $\text{Re} = \dfrac{U_0 L}{\upsilon}$ is the Reynolds number.

Results and Discussion

Here, Eqs. (9-11) subject to the boundary conditions, Eqs. (12) and (13), were solved numerically using Maple 14. This software uses a sixth order Runge-Kutta-Fehlberg method as the default method to solve the boundary value problems numerically. Its accuracy and robustness have been repeatedly confirmed in our previous publications [24-28]. As a further check on the accuracy of our numerical computations, we compare our results with Reddy and Reddy [22] in Table 1 and excellent agreement was established. These results pertain to a circumstance when the Eckert number *Ec, Dufour number Df, Soret number Sr, Chemical reaction parameter λ* and order of chemical reaction *n were* absent. Table 2 has been prepared to illustrate the effects of embedded flow parameters on the skin-friction, the Nusselt number and the Sherwood number. It is seen that as heat generation parameter Q and Dufour number increases Df, there is an increases in the skin-friction coefficient, the Nusselt number and the Sherwood number. An increase in the Soret number Sr, the order of chemical reaction n and the Soret number Sr, there is a fall in the skin-friction and the Nusselt number but the Sherwood number increases. Similarly, increasing the radiation parameter Ra brings a decrease in the skin-friction coefficient, Nusselt number and the Sherwood number. Increase in the Eckert number Ec brings a fall in the skin-friction coefficient and increases in the Nusselt number and Sherwood number. Finally, as the chemical reaction parameter λ increases, the skin-friction coefficient and the Nusselt number increases while the Sherwood number decreases across the plate.

We now turn out attention to the discussion of graphical results that provide additional insights into the problem under consideration.

Graphical Results

A representative set of numerical results is shown graphically in Figures 1-19, to illustrate the effect of the embedded physical flow parameters on the velocity, temperature and concentration profiles. In this study, the value of Pr is chosen to be 0.71, which corresponds to air and the value of Sc is chosen to be 0.22 which represent hydrogen at 25°C and 1 atm. Attention is focused on positive values of the buoyancy parameters i.e. Grashof number Gt > 0 (which corresponds to the cooling problem) and solutal Grashof number Gc > 0 (which indicates that the chemical species concentration in the free stream region is less than the concentration at the boundary surface). The cooling problem is often encountered in engineering applications; for example in the cooling of electronic components and nuclear reactors. Du = 0.03 ,Sr = 2 (i.e. SrDu = 0.06), M = 0.1, g_s = 1, g_c = 0.1 which represents physically buoyant hydrogen diffusing in a weakly magnetoaerodynamic boundary layer convection flow through a highly porous medium with Soret and Dufour effects present.

For various values of thermal Grashof number g_s, the velocity and the temperature profiles are plotted in Figures 1 and 2. It can be seen that as g_s increases, there is a sudden increase close to the wall plate and the velocity and thermal boundary layer thickness thickens before obeying the boundary conditions. Similar effects were observed for the influence of solutal Grashof number g_c (see Figures 3 and 4). Figures 5 and 6 represent the effect of permeability parameter K on the velocity and the temperature profiles. It is seen that the velocity and the thermal boundary layer thickness reduces as the permeability parameter increases which agrees with the existing literature. Figure 7 shows the effect of magnetic field parameter M on the velocity profiles. It was observed that as M increases, the velocity decreases. This result qualitatively agrees with the expectations, since the magnetic field exerts a retarding force on the flow. For various values of the radiation parameter Ra, the velocity and temperature profiles are plotted in Figures 8 and 9. It can be seen that as Ra increases, the velocity and thermal boundary layer thickness thicken away from the wall plate. It is seen from Figures 10 and 11, as the heat generation parameter Q increases, the heat is generated the buoyancy force increases which induces the flow rate to increase giving rise to the increase in the velocity and temperature profiles. Generally, increasing the heat generation parameter thickens the velocity and the thermal boundary layer thickness. Figures 12 and 13 represent the effect of Eckert number Ec on the velocity and temperature profiles.

It can be seen that increasing Ec enhances the fluid flow which thickens the velocity and thermal boundary layer thickness across the plate. The effects of Dufour number Df on the velocity and temperature profiles were displayed in Figures 14 and 15. It has profound influence on both profiles. Increasing Dufour number thickens the velocity and thermal boundary layer thickness. In Figure 16, as the chemical reaction parameter λ increases, the concentration boundary layer thickness decreases across the channel. It can be seen from Figure 17 that increasing the order of chemical reaction n enhances the concentration profile. Figure 18 represents the effect of Schmidt number Sc on the concentration profile. Increasing the Sc thinning the concentration boundary layer thickness as expected. Figures 19 and 20 show the effect of suction on the velocity and concentration profiles. Suction steps down flow and causes a reduction in the concentration of the fluid. Figure 21 represents the influence of Soret number Sr on the concentration profiles. Increasing Soret number Sc enhances the concentration of the fluid as expected.

Table 1: Comparison results for Sherwood number Sh for M = 0.1, K = 0.05, g_s = 1.0, g_c = 0.1, Pr = 0.71, Ra = 0.5, Q = 0.5 and fw for various values for Schmitz number Sc in the absent of *Ec, Df, Sr, λ* and *n*

Sc	**Reddy and Reddy [22] Sh**	**Present result Sh**
0.3	0.333777	0.335999401355351
0.6	0.475483	0.487199262289322
0.71	0.521061	0.534003141890994
1.0	0.630434	0.645468003415921

Table 2: Numerical values of the skin-friction C_f, Nusselt number Nu and Sherwood number Sh for M = 0.1, K = 0.05, g_s = 1.0, g_c = 0.1, fw = 0.5 and Pr = 0.71

Ra	Q	Sc	Df	Sr	Ec	λ	n	$f''(0)$	$\theta'(0)$	$-\phi(0)$
0.1	0.5	0.22	0.03	2	2	0.1	1	2.4764465926	3.056097621	1.666987461
0.3	0.5	0.22	0.03	2	2	0.1	1	2.4253256300	2.410396774	1.387665331
0.5	0.5	0.22	0.03	2	2	0.1	1	2.3840140577	1.972440815	1.198973841
0.1	0.6	0.22	0.03	2	2	0.1	1	2.7576759265	4.007787875	2.077070034
0.1	0.7	0.22	0.03	2	2	0.1	1	3.0322801358	5.018206414	2.546136894
0.1	0.5	0.62	0.03	2	2	0.1	1	2.4163026195	2.978540690	4.189266668
0.1	0.5	0.78	0.03	2	2	0.1	1	2.4010159973	2.969365910	5.173393640
0.1	0.5	0.22	0.15	2	2	0.1	1	2.5140567819	3.261735941	1.756630766
0.1	0.5	0.22	0.60	2	2	0.1	1	2.6731897260	4.223938564	2.175773889
0.1	0.5	0.22	0.03	3	2	0.1	1	2.4633675108	3.040889496	2.345922274
0.1	0.5	0.22	0.03	5	2	0.1	1	2.4384782446	3.013968767	3.688614648
0.1	0.5	0.22	0.03	2	4	0.1	1	1.7408147717	2.105043275	1.685257465
0.1	0.5	0.22	0.03	2	5	0.1	1	1.8760176461	3.177029632	2.159526783
0.1	0.5	0.22	0.03	2	7	0.1	1	2.3662230685	7.267261095	3.966700137
0.1	0.5	0.22	0.03	2	2	0.5	1	2.5022873512	3.117605570	1.551868452
0.1	0.5	0.22	0.03	2	2	1.0	1	2.5688639540	3.280363439	1.301150639
0.1	0.5	0.22	0.03	2	2	0.1	3	2.4725179125	3.046794529	1.683259787
0.1	0.5	0.22	0.03	2	2	0.1	5	2.4718858066	3.045310389	1.686928930
0.1	0.5	0.22	0.03	2	2	0.1	10	2.4717267265	3.044959976	1.688801493
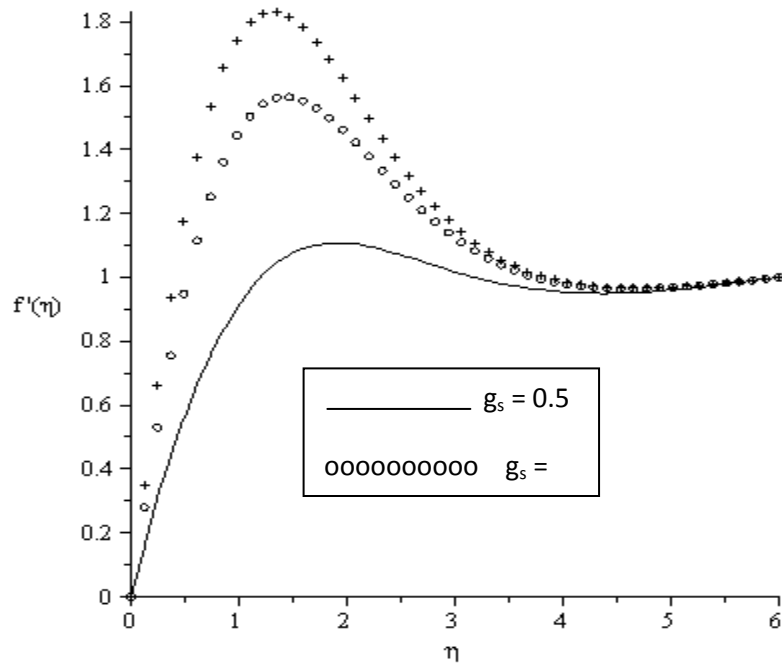
Figure 1: Effects of thermal Grashof number g_s on the velocity profile for fixed values of Pr = 0.71, Sc = 0.22, Df = 0.03, Sr = 2, Ec = 2, λ = 0.1, g_c = 0.1, M = 0.1, K = 0.05, Q = 0.5, fw = 0.5, Ra = 0.1, n = 1.
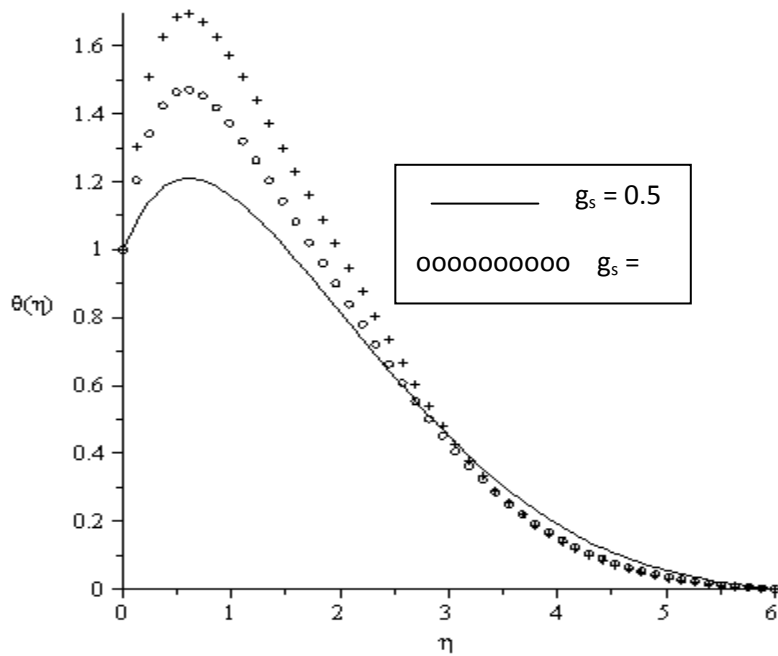
Figure 2: Effects of thermal Grashof number g_c on the temperature profile for fixed values of Pr = 0.71, Sc = 0.22, Df = 0.03, Sr = 2, Ec = 2, λ = 0.1, g_c = 0.1, M = 0.1, K = 0.05, Q = 0.5, fw = 0.5, Ra = 0.1, n = 1.
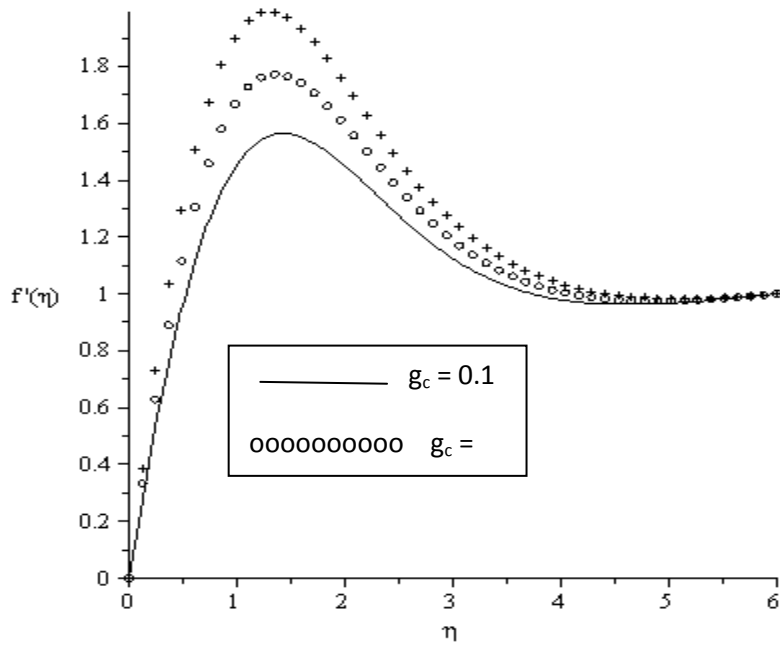
Figure 3: Effects of solutal Grashof number g_c on the velocity profile for fixed values of Pr = 0.71, Sc = 0.22, Df = 0.03, Sr = 2, Ec = 2, λ = 0.1, g_s = 1.0, M = 0.1, K = 0.05, Q = 0.5, fw = 0.5, Ra = 0.1, n = 1.
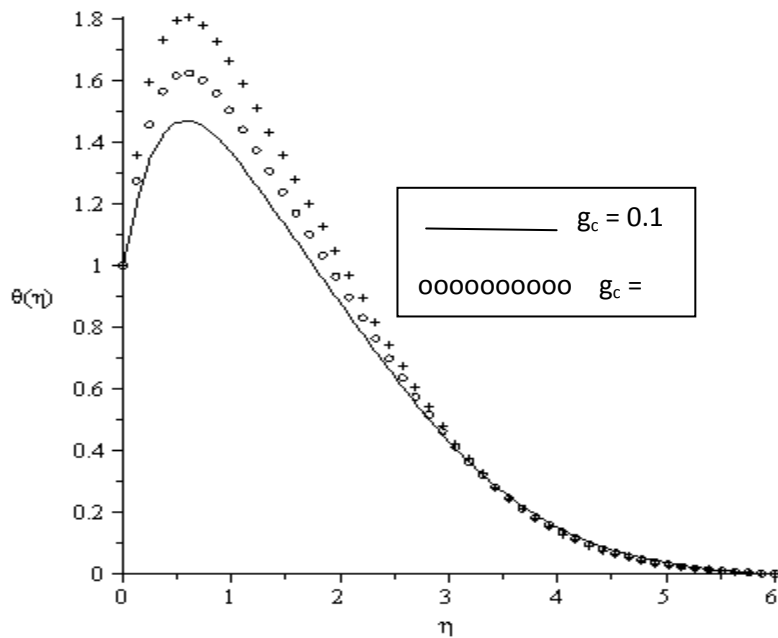
Figure 4: Effects of solutal Grashof number g_c on the temperature profile for fixed values of Pr = 0.71, Sc = 0.22, Df = 0.03, Sr = 2, Ec = 2, λ = 0.1, g_s = 1.0, M = 0.1, K = 0.05, Q = 0.5, fw = 0.5, Ra = 0.1, n = 1.
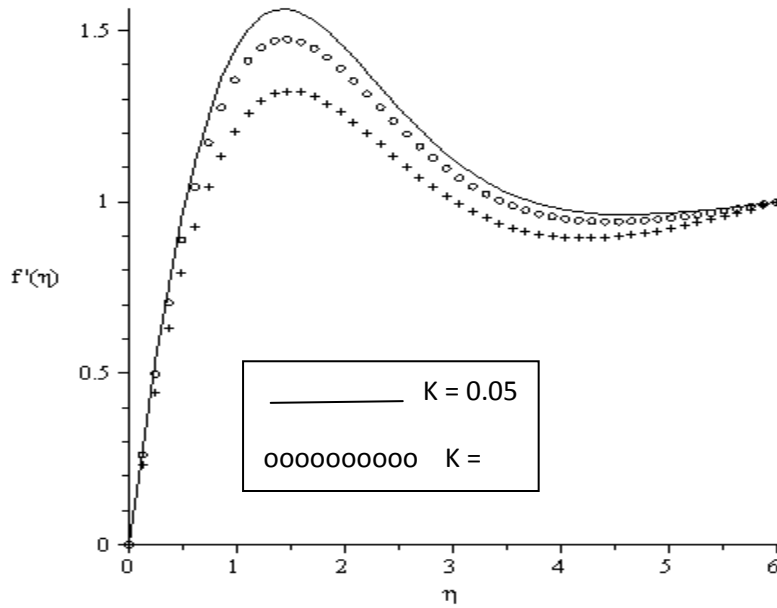
Figure 5: Effects of permeability parameter K on the velocity profile for fixed values of Pr = 0.71, Sc = 0.22, Df = 0.03, Sr = 2, Ec = 2, λ = 0.1, g_s = 1.0, M = 0.1, g_c = 0.1, Q = 0.5, fw = 0.5, Ra = 0.1, n = 1.
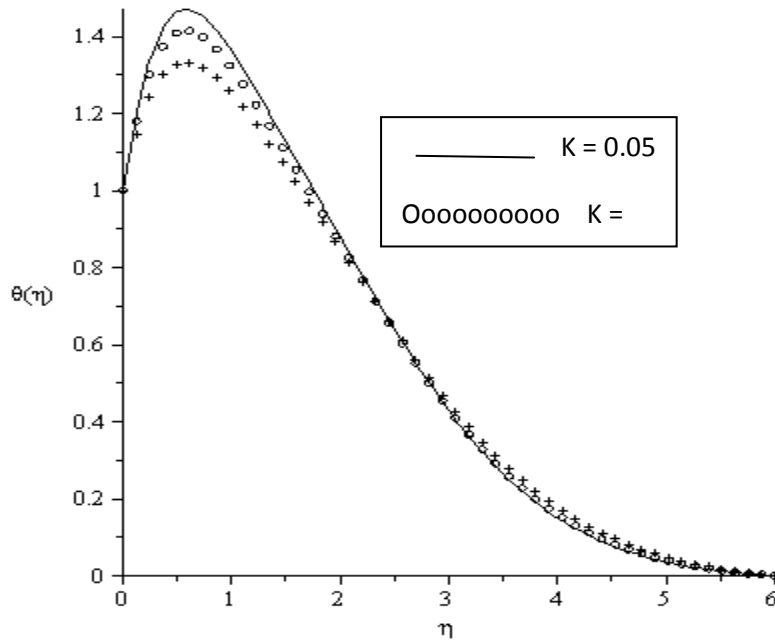
Figure 6: Effects of permeability parameter K on the velocity profile for fixed values of Pr = 0.71, Sc = 0.22, Df = 0.03, Sr = 2, Ec = 2, λ = 0.1, g_s = 1.0, M = 0.1, g_c = 0.1, Q = 0.5, fw = 0.5, Ra = 0.1, n = 1.
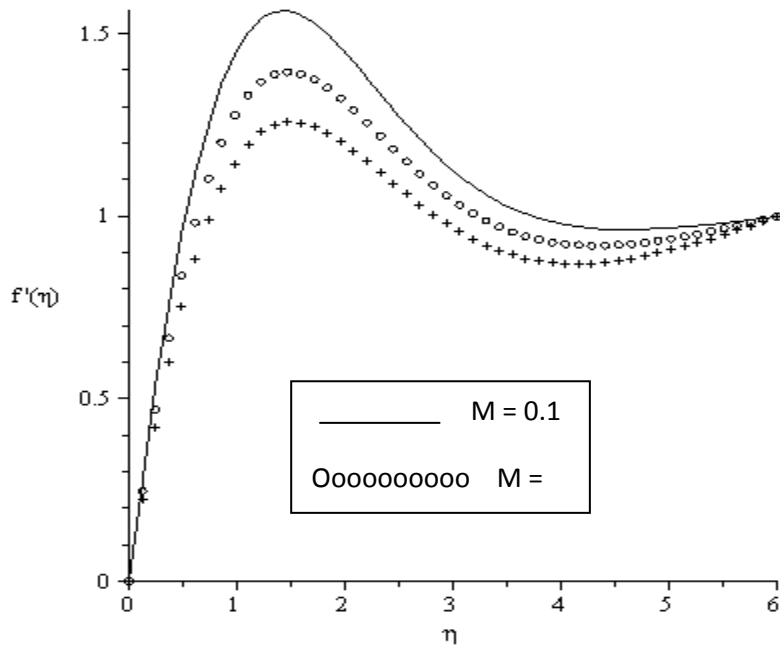
Figure 7: Effects of magnetic field parameter M on the velocity profile for fixed values of Pr = 0.71, Sc = 0.22, Df = 0.03, Sr = 2, Ec = 2, λ = 0.1, g_s = 1.0, K = 0.05, g_c = 0.1, Q = 0.5, fw = 0.5, Ra = 0.1, n = 1.
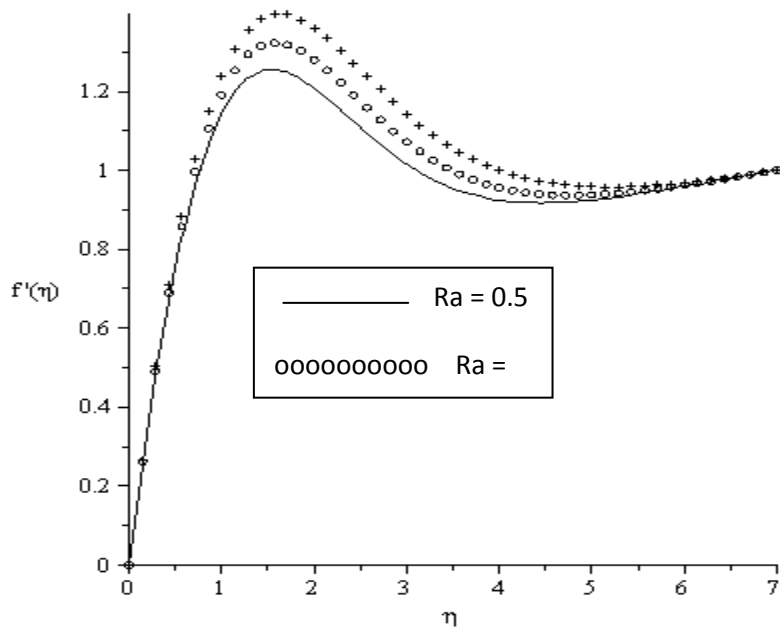
Figure 8: Effects of thermal radiation parameter Ra on the velocity profile for fixed values of Pr = 0.71, Sc = 0.22, Df = 0.03, Sr = 2, Ec = 2, λ = 0.1, g_s = 1.0, K = 0.05, g_c = 0.1, Q = 0.5, fw = 0.5, M = 0.1, n = 1.
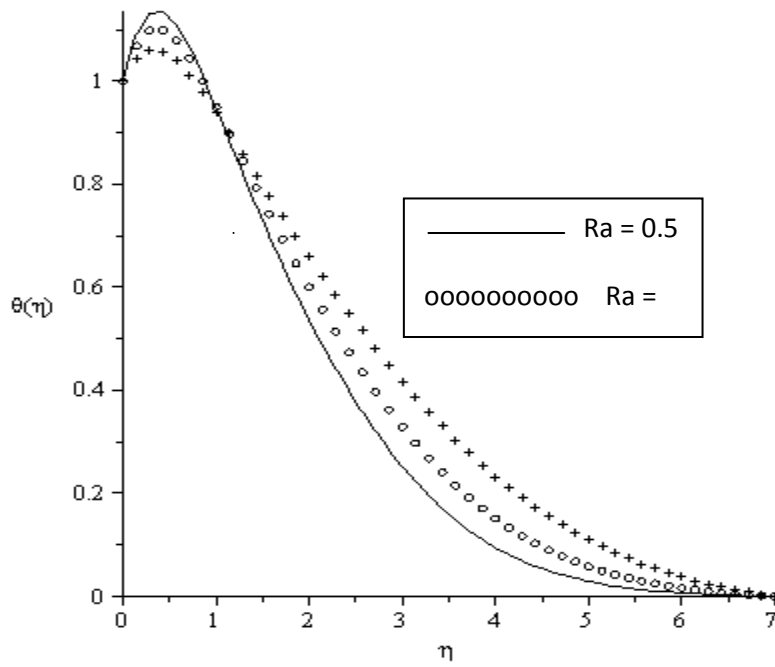
Figure 9: Effects of thermal radiation parameter Ra on the temperature profile for fixed values of Pr = 0.71, Sc = 0.22, Df = 0.03, Sr = 2, Ec = 2, λ = 0.1, g_s = 1.0, K = 0.05, g_c = 0.1, Q = 0.5, fw = 0.5, M = 0.1, n=1.
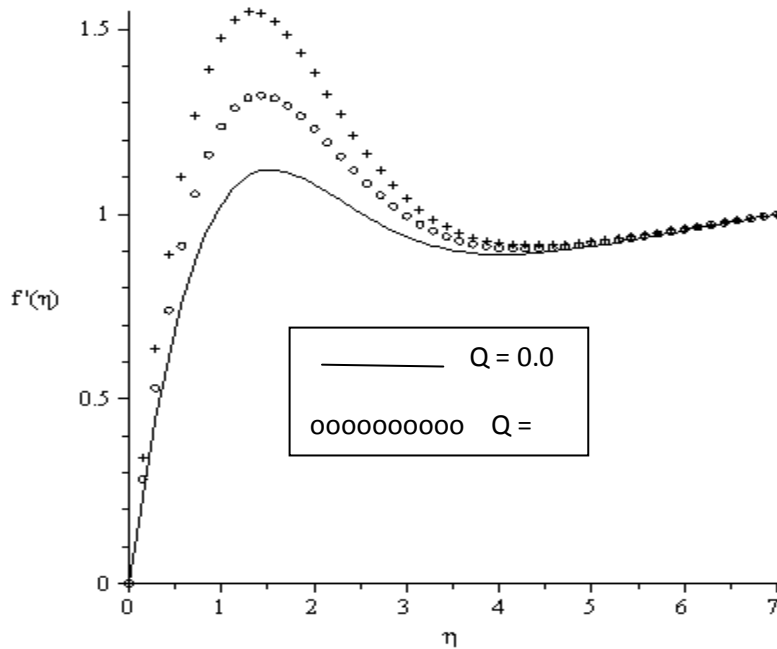
Figure 10: Effects of internal heat generation Q on the velocity profile for fixed values of Pr = 0.71, Sc = 0.22, Df = 0.03, Sr = 2, Ec = 2, λ = 0.1, g_s = 1.0, K = 0.05, g_c = 0.1, Ra = 0.1, fw = 0.5, M = 0.1, n = 1.
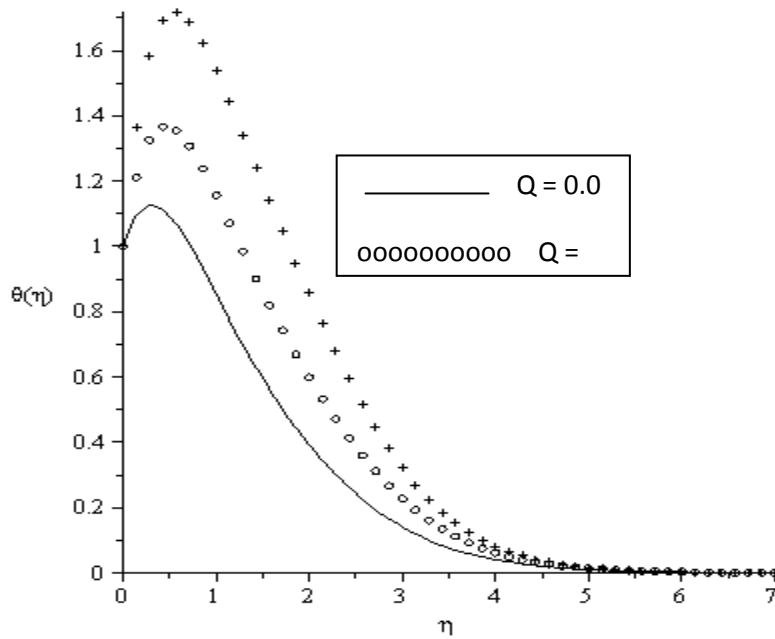
Figure 11: Effects of internal heat generation Q on the temperature profile for fixed values of Pr = 0.71, Sc = 0.22, Df = 0.03, Sr = 2, Ec = 2, λ = 0.1, g_s = 1.0, K = 0.05, g_c = 0.1, Ra = 0.1, fw = 0.5, M = 0.1, n = 1.
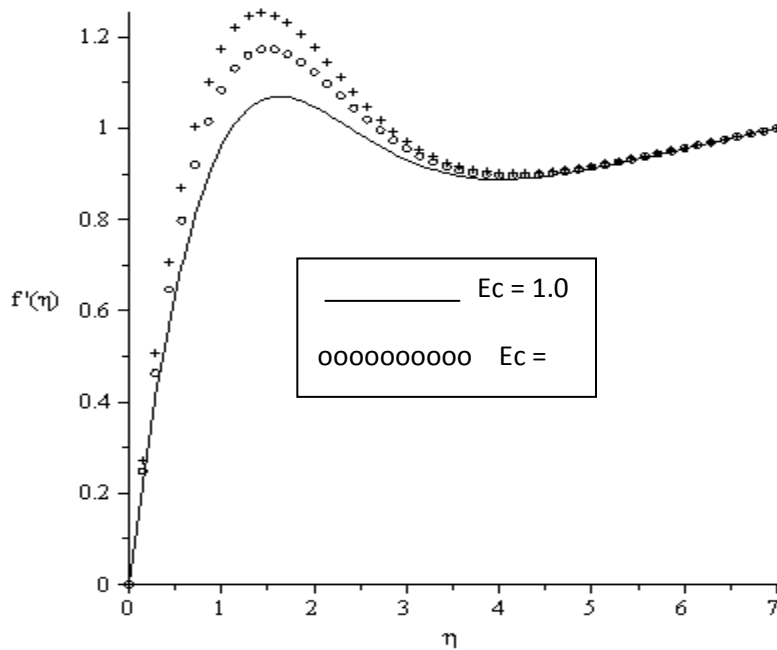
Figure 12: Effects of Eckert number Ec on the velocity profile for fixed values of Pr = 0.71, Sc = 0.22, Df = 0.03, Sr = 2, Q = 0.1, λ = 0.1, g_s = 1.0, K = 0.05, g_c = 0.1, Ra = 0.1, fw = 0.5, M = 0.1, n = 1.
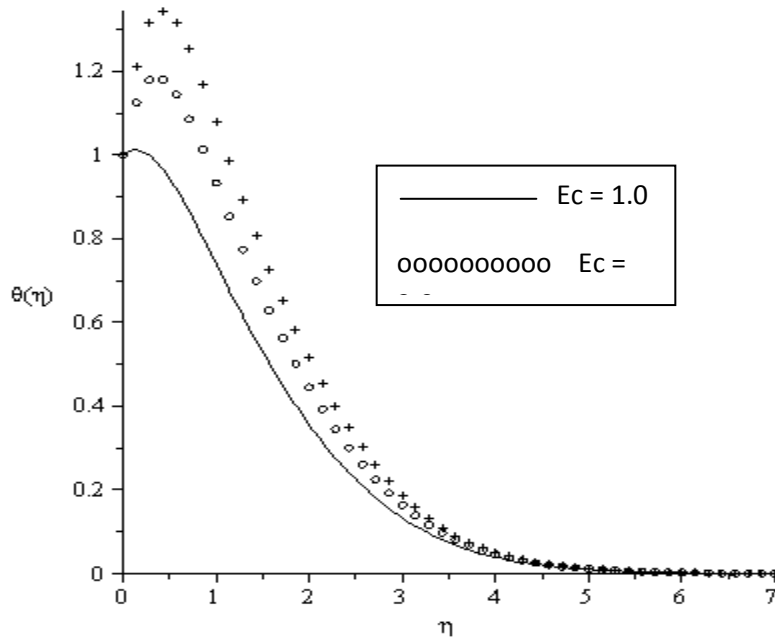
Figure 13: Effects of Eckert number Ec on the velocity profile for fixed values of Pr = 0.71, Sc = 0.22, Df = 0.03, Sr = 2, Q = 0.1, λ = 0.1, g_s = 1.0, K = 0.05, g_c = 0.1, Ra = 0.1, fw = 0.5, M = 0.1, n=1.
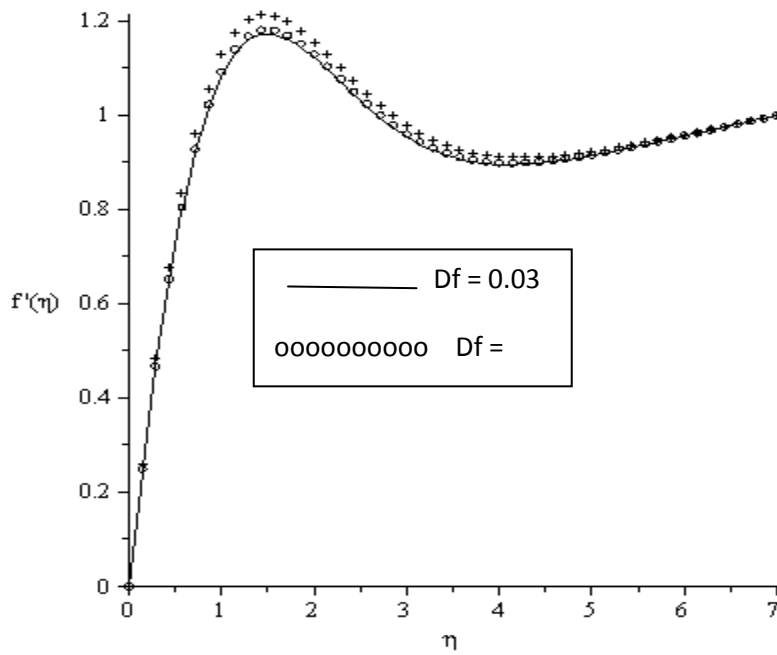
Figure 14: Effects of Dufour number Df on the velocity profile for fixed values of Pr = 0.71, Sc = 0.22, Ec = 2, Sr = 2, Q = 0.1, λ = 0.1, g_s = 1.0, K = 0.05, g_c = 0.1, Ra = 0.1, fw = 0.5, M = 0.1, n = 1.
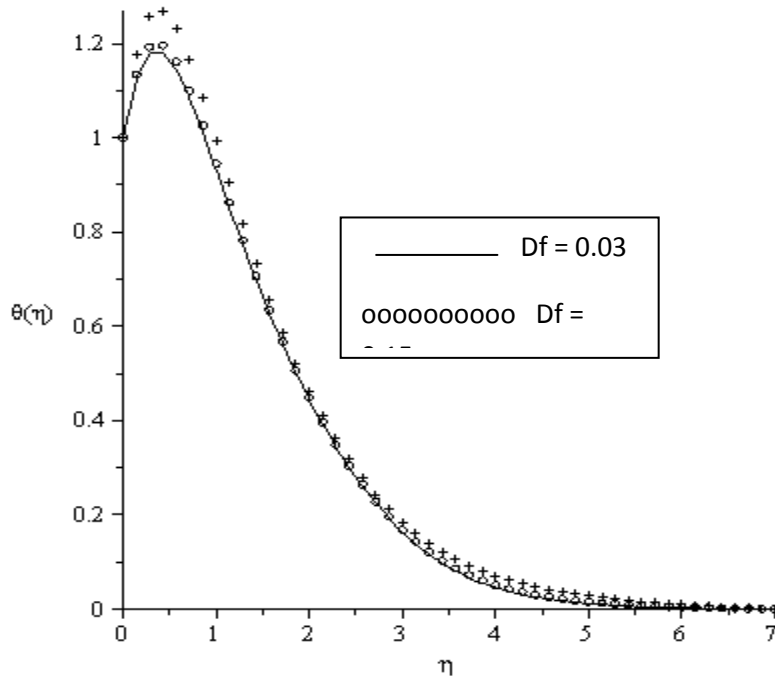
Figure 15: Effects of Dufour number Df on the temperature profile for fixed values of Pr = 0.71, Sc = 0.22, Ec = 2, Sr = 2, Q = 0.1, λ = 0.1, g_s = 1.0, K = 0.05, g_c = 0.1, Ra = 0.1, fw = 0.5, M = 0.1, n = 1.
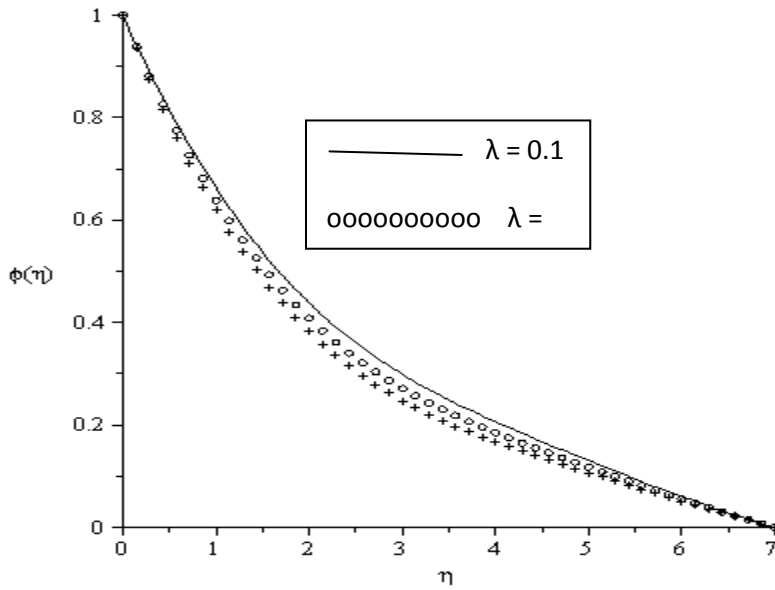
Figure 16: Effects of chemical reaction parameter λ on the concentration profile for fixed values of Pr = 0.71, Sc = 0.22, Df = 0.03, Sr = 2, Q = 0.5, Df = 0.03, g_s = 0.1, K = 0.05, g_c = 0.1, Ra = 0.1, fw = 0.5, M = 0.2, n = 1.
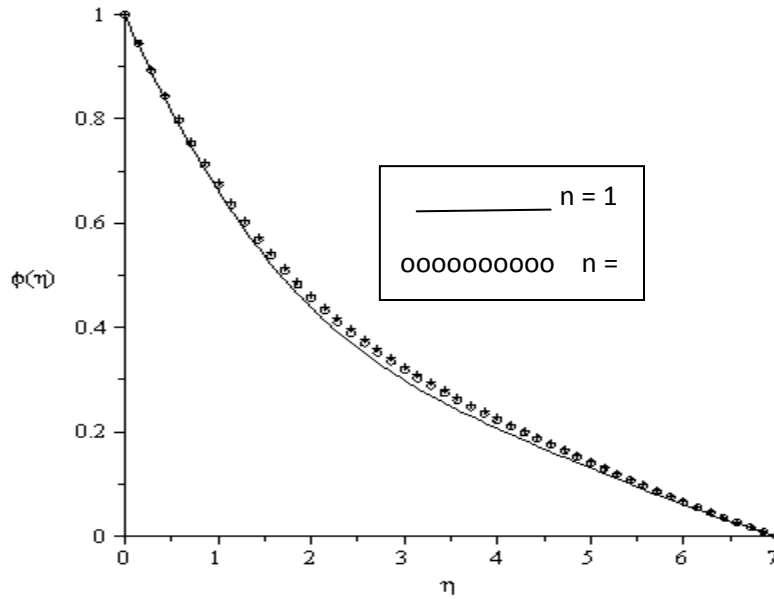
Figure 17: Effects of order of chemical reaction parameter n on the concentration profile for fixed values of Pr = 0.71, Sc = 0.22, Df = 0.03, Sr = 1, Q = 0.5, Df = 0.03, g_s = 1.0, K = 0.05, g_c = 0.1, Ra = 0.1, fw = 0.5, M = 0.1, λ = 0.1.
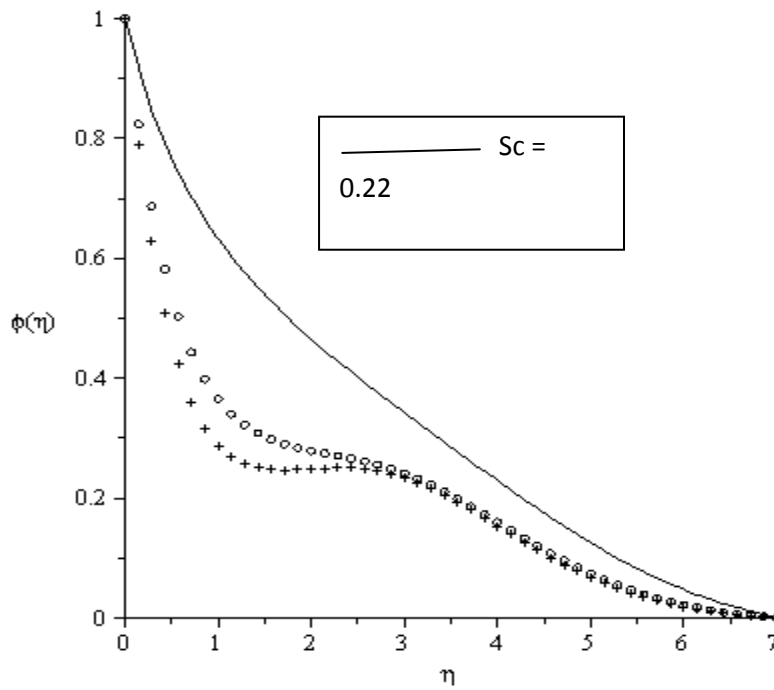
Figure 18: Effects of Schmidt number Sc n on the concentration profile for fixed values of Pr = 0.71, n = 1, Df = 0.03, Sr = 1, Q = 0.5, Df = 0.03, g_s = 1.0, K = 0.05, g_c = 0.1, Ra = 0.1, fw = 0.5, M = 0.1, λ = 0.1.
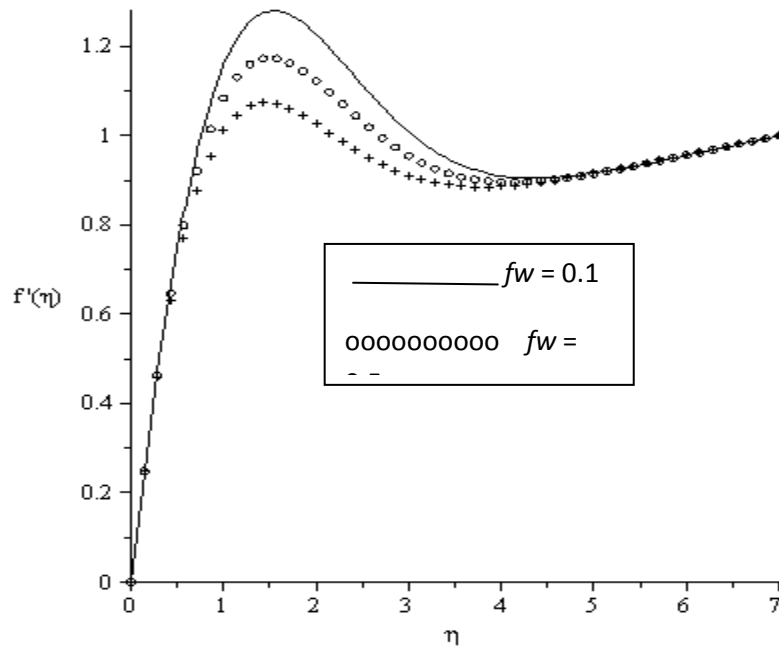
Figure 19: Effects of suction fw on the velocity profile for fixed values of Pr = 0.71, Sc = 0.22, Ec = 2, Sr = 2, Q = 0.1, λ = 0.1, g_s = 1.0, K = 0.05, g_c = 0.1, Ra = 0.1, Df = 0.03, M = 0.1, n = 1.
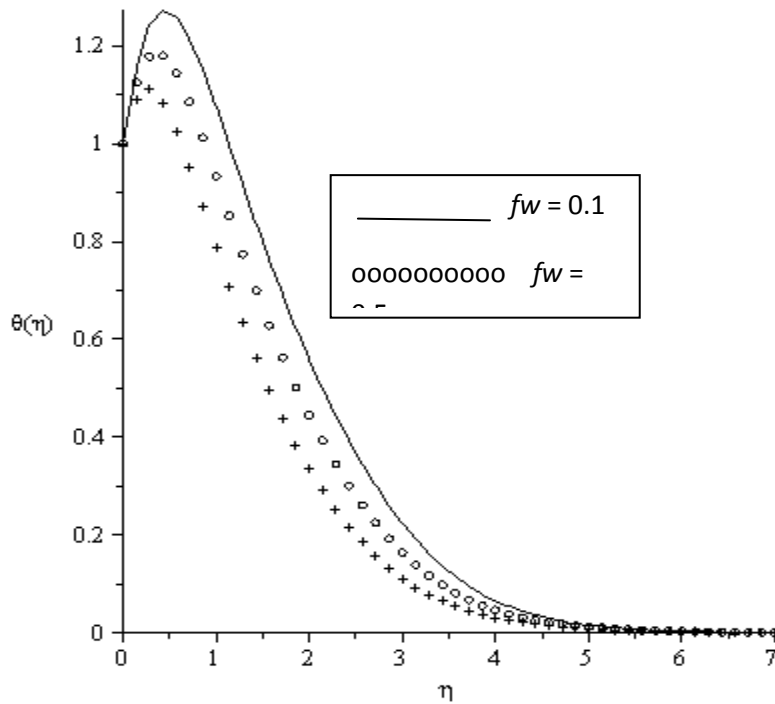
Figure 20: Effects of suction fw on the temperature profile for fixed values of Pr = 0.71, Sc = 0.22, Ec = 2, Sr = 2, Q = 0.1, λ = 0.1, g_s = 1.0, K = 0.05, g_c = 0.1, Ra = 0.1, Df = 0.03, M = 0.1, n = 1.
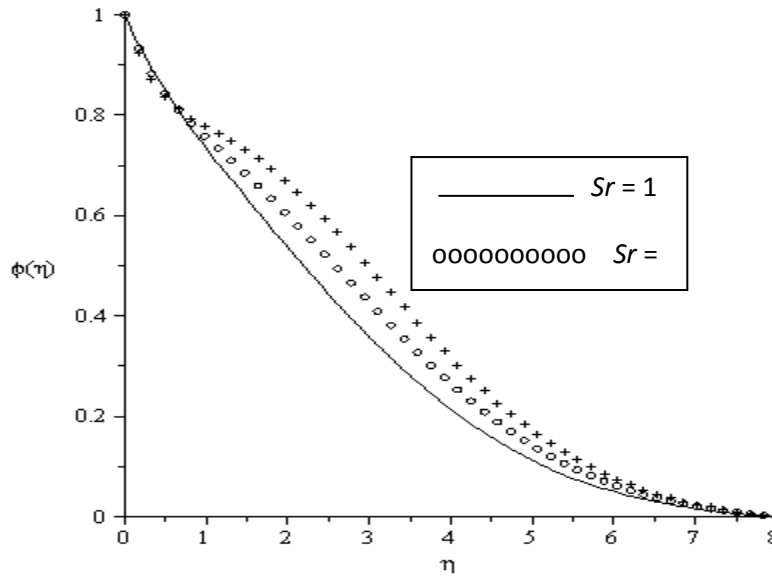
Figure 21: Effects of Soret number Sr n on the concentration profile for fixed values of Pr = 0.71, n = 1, Df = 0.03, Sc = 0.22, Q = 0.1, Df = 0.03, g_s = 1.0, K = 0.05, g_c = 0.1, Ra = 0.1, fw = 0.5, M = 0.1, λ = 0.1.

Conclusions

Numerical solutions are obtained for the effects of thermal diffusion and diffusion thermo on MHD combined convection and mass transfer past a vertical porous plate embedded in a porous medium with heat generation, thermal radiation, nth order chemical reaction and viscous dissipation. Employing similarity transformation technique, the governing equations are transformed into ordinary differential equations and solve numerically by the shooting method. We present results to illustrate the flow characteristics for the velocity, temperature and concentration fields as well as the skin friction, heat and mass transfer, and show how the flow fields are influenced by the material parameters of the flow problem. We observed that increase in Dufour number *Df*, Eckert number Ec and chemical reaction parameter *λ* leads to an increase in the heat transfer coefficient and the mass transfer coefficient except for *λ*. Increases the order of chemical reaction parameter n brings a decrease to heat transfer rate and enhances the mass transfer rate. We noticed that the temperature increases while the concentration profile decreases with increasing *Ec* and *Sc*. We conclude that for fluids with medium molecular weight (H_2, air), the thermal-diffusion and diffusion-thermo as well as viscous dissipation, thermal radiation and order of chemical reaction including internal heat generation with suction on a viscous incompressible electrically conducting and radiating fluid should not be neglected.

Acknowledgement

References

1. J S Turner, Buoyancy Effects in Fluids, Cambridge University Press, London, 1973

2. J S Turner, Double diffusive phenomena, Annu. Rev. Fluid Mech. (1974) 6 37–56.

3. J S Turner, Multicomponent convection, Annu. Rev. Fluid Mech. (1985) 17 11–44.

4. H E Huppert, J S Turner, Double diffusive convection, J. Fluid Mech. (1981) 106 299–329.

5. J K Platten, J C Legros, Convection in Liquids, Springer, Berlin, 1984.

6. T J Mc Dougall, Double diffusive convection caused by coupled molecular diffusion, J. Fluid Mech. (1982) 126 379–397.

7. N Rudraiah, M S Malashetty, The influence of coupled molecular diffusion on double diffusive convection in a porous medium, ASME J. Heat Transfer(1986) 108 872–878.

8. N Rudraiah, P.G. Siddheshwar, A weak nonlinear stability analysis of double diffusive convection with cross-diffusion in a fluid saturated porous medium, Heat Mass Transfer (1998) 33 111-135

9. E M Sparrow, W J Minkowycz, E.R.G. Eckert, Transpiration-induced buoyancy and thermal diffusion–diffusion thermo in a helium air free convection boundary layer, J. Heat Transfer(1964) 86 508–514.

10. E M Sparrow, W J Minkowycz, E.R.G. Eckert, Diffusion-thermo in a stagnation-point flow of air with injection of gasses of various molecular weights in the boundary layer, AIAA J. (1964) 2 652–659.

11. O E Tewfik, J W Yang, The thermodynamic coupling between heat and mass transfer in free convection, Int. J. Heat Mass Transfer(1963) 6 915–922.

12. O.E. Tewfik, R.R.G. Eckert, L.S. Jurewicz, Diffusion-thermo effects on heat transfer from a cylinder in cross-flow, AIAA J. (1963) 1 1537–1543.

13. E R G Eckert, R M Drake, Analysis of Heat and Mass Transfer, Mc Graw-Hill, New York, 1972.

14. A T Atimtay, W N Gill, The effect of free stream concentration on heat and binary mass transfer with thermodynamic coupling in convection on a rotating disc, Chem. Eng. Commun. (1985) 34 161–185.

15. J.A. Weaver, R. Viskanta, Natural convection due to horizontal temperature and concentration gradients—1. Variable thermo physical property effects, Int. J. Heat Mass Transfer (1991) 34 3107–3120.

16. N G Kafoussias, E M Williams, Thermo-diffusion and diffusion-thermo effects on mixed free-forced convective and mass transfer boundary layer flow with temperature dependent viscosity, Int. J. Eng. Sci. (1995) 33 1369–1384.

17. E Knobloch, Convection in binary fluids, Phys. Fluids (1980) (9) 1918–1920.

18. Emmanuel Osalusi, Jonathan Side, Robert Harris, thermal-diffusion and diffusion-thermo effects on combined heat and mass transfer of a steady MHD convective and slip flow due to a rotating disk with viscous dissipation and Ohmic heating, Int. Commun in heat and mass transfer (2008) 35 908-915.

19. O Anwar Beg, A Y Bakier, V R Prasad, Numerical study of free convection magnetohydrodynamic heat and mass transfer from a stretching surface to a saturated porous medium with Soret and Dufour effects, Computational material science (2009) 46 57-65.

20. Ahmed A Afify, similarity solution in MHD: effects of thermal diffusion and diffusion thermo on free convective heat and mass transfer over a stretching surface considering suction or injection, Commun Nonlinear Sci Numer Simulat (2009) 14 2202-2214.

21. T Hayat, M Mustafa, I Pop, heat and mass transfer for Soret and Dufour's effect on mixed convection boundary layer flow over a stretching vertical surface in a porous medium filled with a viscoelastic fluid, Commun Nonlinear Sci Numer Simulat (2010) 15 1183-1196.

22. P Bala Anki Reddy, N Bhaskar Reddy, Radiation effects on MHD combined convection and mass transfer flow past a vertical porous plate embedded in a porous medium with heat generation, Int. J. of Appl. Math and Mech. , 2010 6 (18): 33-49.

23. M Q Brewster, Thermal radiative transfer and properties, John Wiley & Sons, New York. (1992)

24. A Aziz, "A similarity solution for laminar thermal boundary over a flat plate with a convective boundary condition," Commun. Nonlinear Sci. Numer. Simulat. (2009) 14, 1064-1068

25. O D Makinde, P O Olanrewaju, "Buoyancy effects on thermal boundary layer over a vertical plate with a convective surface boundary condition," Trans. ASME - J. Fluids Eng. (2010) 132, 044502(1-4)

26. P O Olanrewaju, J A Gbadeyan, T Hayat, A A Hendi, "Effects of internal heat generation, thermal radiation and buoyancy force on a boundary layer over a vertical plate with a convective surface boundary condition," S Afri J Sci. 2011; 107 (7/8). Doi:10.4102/sajs.v107i7/8.476

27. P O Olanrewaju, Z Abbas, Corrigendum to Convection heat and mass transfer in a hydromagnetic flow of a second grade fluid in the presence of thermal radiation and thermal diffusion[Int. J. Heat Mass Transf. 38 (3) (2011) 377-382], *International Communications in Heat and Mass Transfer(2014) 51 59-60.*

28. P O Olanrewaju , F I, Alao, A Adeniyan, , Effects of thermal-diffusion, diffusion thermo, magnetic field and viscous dissipation on unsteady mixed convection flow past a porous plate moving through a binary mixture of chemically reacting fluid, *Thermal Energy and Power Engineering(2013) Vol. 2 118-131.*